

Structure of Liquid Water Determined from Infrared Temperature Profiling and Evolutionary Curve Resolution

F. O. Libnau, J. Toft, A. A. Christy, and O. M. Kvalheim*

Contribution from the Department of Chemistry, University of Bergen, N-5007 Bergen, Norway

Received January 18, 1994. Revised Manuscript Received June 1, 1994*

Abstract: By utilizing the evolving nature of liquid water subjected to controlled heating, mid-infrared profiles acquired in the interval 2–96 °C are resolved into two spectra that can be interpreted as representing an equilibrium between two water structures differing in the average number of H bonds per water molecule. The structure with the lower number of H bonds is increasing with increasing temperature at the expense of the other. Assuming that the structures differ on the average of half a H bond per water molecule, the enthalpy and entropy change for the transformation from the stronger to the lesser H bonded structure were calculated as 2.2 kcal mol⁻¹ and 7.3 cal mol⁻¹ K⁻¹. This is in excellent agreement with previously reported results for a transformation of water clusters consisting of polycyclic octamers or decamers into clusters of monocyclic tetramers or pentamers.

Without comparison, water is the most studied system in chemistry. Despite this fact, water is still far from being satisfactorily described on the molecular level and continues to fascinate new generations of chemists. This situation reflects the difficulty of providing a structural description that accounts for the dynamic behavior of the H bonding ability of water, *i.e.*, the ability of water molecules to form structures of collective character.

Different models describing the water structure may be divided into two main classes: mixture and continuum models.^{1,2} The former indicates an equilibrium mixture of discrete species, differing according to their specific structural arrangements. The latter suggests almost completely H bonded molecules in a continuous network where distortion of the H bonds results in a continuous distribution of H bond distances, angles, and energies. Using Raman and near-infrared respectively, Walrafen *et al.*^{3–6} and Luck⁷ (and references therein) interpret their experimental data in terms of an equilibrium mixture with varying degrees of discrete water entities. According to Walrafen,⁸ liquid water contains three structural components: four-, three-, and two-coordinated H bonded entities. In order to calculate the H bond enthalpy, the same authors use a two-state approach in which water is partitioned into H bonded and non-H bonded entities. Recently, Benson and Siebert⁹ proposed a two-component equilibrium where a polycyclic octamer dissociates into two monocyclic tetramers or a polycyclic decamer dissociates into two monocyclic pentamers.

Among others, Franck and Roth,¹⁰ Ratcliffe and Irish,¹¹ and Efimov and Naberukhin¹² tend to interpret their results in favor of a continuum. Efimov and Naberukhin have calculated the band shape of H₂O and D₂O in the stretching vibration region

and stated that "It is not necessary to postulate the existence of discrete species of aggregates nor the displacement of the equilibrium between them in the liquid." They attributed the temperature dependent changes to Fermi resonance between the stretching vibrations and the overtone of the bending vibrations. This explanation has been disputed by Walrafen.⁴

The description of liquid water in terms of a closed two-state system has recently found support in Raman studies by Hare and Sorenson^{13–15} and mid-infrared studies by Maréchal¹⁶ using the attenuated total reflection (ATR) technique. However, no decisive conclusions were possible from these studies. The number of coexisting water species therefore remains an open question.

As pointed out by Maréchal,¹⁶ mid-infrared spectroscopy, which may be expected to be the most powerful technique in the study of H bonding character in liquid water, has been almost absent from the repertoire of chemists investigating the water structure. The main reason for this is the strong absorbance of the fundamental OH stretching giving rise to intense broad bands prohibiting reliable quantitative structural information from this region with standard infrared techniques. New techniques such as ATR have changed the situation and, as shown by Maréchal,¹⁶ high-quality spectra of the mid-infrared region can be obtained.

Paralleling the instrumental development, new data-analytical techniques for mixture analysis have become available¹⁷ (and references therein). While the old curve resolution methods make many uncontrollable assumptions, many of the new methods need very few or no assumptions at all. Thus, the procedure of decomposing spectral bands into a number of Gaussian bands, without knowledge of the true number of species contributing to a composite band, represents a common but uncontrollable approach that may provide misleading results, especially in the absence of precise estimates of the noise level. Since the procedure is available in most data-processing packages delivered by instrument manufacturers, it is not surprising that the approach has been attempted for resolving bands in water spectra.^{4,7} On the other hand, by taking advantage of the evolving nature of the spectroscopic data acquired from a system subjected to continuously increasing temperature, no assumptions are necessary regarding the number of species or peak shape in the resolution process. Instead this information is extracted directly from the matrix of spectroscopic data defined by temperature and

* Abstract published in *Advance ACS Abstracts*, August 1, 1994.

(1) Eisenberg, D.; Kauzmann, W. *The Structure and Properties of Water*; Oxford University Press: London, 1969.

(2) Némethy, G. In *Structure of Water and Aqueous Solutions*; Luck, W. A. P., Ed.; Verlag Chemie: Weinheim/Bergstr., 1974; p 73.

(3) Walrafen, G. E.; Hokmabadi, M. S.; Yang, W.-H. *J. Chem. Phys.* **1986**, *85*, 6964.

(4) Walrafen, G. E.; Fisher, M. R.; Hokmabadi, M. S.; Yang, W.-H. *J. Chem. Phys.* **1986**, *85*, 6970.

(5) Walrafen, G. E.; Hokmabadi, M. S.; Yang, W.-H. *J. Chem. Phys.* **1988**, *92*, 2433.

(6) Walrafen, G. E.; Hokmabadi, M. S.; Yang, W.-H.; Chu, Y. C. *J. Phys. Chem.* **1989**, *93*, 2909.

(7) Luck, W. A. P. in ref 2, p 247.

(8) Walrafen, G. E. In *Water a Comprehensive Treatise*; Franks, F., Ed.; Plenum Press: New York, 1972; Vol. 1, p 208.

(9) Benson, S. W.; Siebert, E. D. *J. Am. Chem. Soc.* **1992**, *114*, 4269.

(10) Franck, E. U.; Roth, K. *Discuss. Faraday Soc.* **1967**, *43*, 108.

(11) Ratcliffe, C. I.; Irish, D. E. *J. Chem. Phys.* **1982**, *86*, 4897.

(12) Efimov, Yu. Ya.; Naberukhin, Yu. I. *Mol. Phys.* **1978**, *36*, 973.

(13) Hare, D. E.; Sorensen, C. M. *J. Chem. Phys.* **1990**, *93*, 25.

(14) Hare, D. E.; Sorensen, C. M. *J. Chem. Phys.* **1990**, *93*, 6954.

(15) Hare, D. E.; Sorensen, C. M. *J. Chem. Phys.* **1992**, *96*, 13.

(16) Maréchal, Y. *Chem. Phys.* **1991**, *95*, 5565.

(17) Liang, Y.-z.; Kvalheim, O. M.; Manne, R. *Chemom. Intell. Lab. Syst.* **1993**, *18*, 235.

wavelength. This is possible by using evolutionary curve resolution methods such as heuristic evolving latent projections¹⁸ and sequential rank analysis¹⁹ which have recently been developed in our laboratory.

The aim of this work is to provide conclusive evidence on the number of distinct structures coexisting in liquid water together with some clues on the composition of these structures. This will be accomplished from ATR infrared measurements resolved by evolutionary curve resolution. Furthermore, we shall report for the first time resolved mid-infrared spectra of the coexisting water structures. From this result, it is possible to calculate enthalpy and entropy change for the equilibrium between the different water structures.

Experimental Section

Water was doubly distilled and de-ionized. Prior to use it was boiled to remove solved gases and, subsequently, when still warm, directly transferred into a circular cell. Attenuated total reflectance (ATR) spectra of water were obtained by using a Nicolet-800 Fourier transform IR spectrometer equipped with a micro Circle-cell providing ca. 5 internal reflections and a mercury-cadmium-telluride (MCT) detector. Spectra were recorded from 4000 to 650 cm^{-1} using 16 scans with optical resolution of 4 cm^{-1} and data point resolution of 2 cm^{-1} . Infrared spectra were acquired from 2 to 96.2 °C in steps of ca. 2 °C. A total of 48 spectra were sampled at a continuous heating rate of 0.6–0.7 °C/min. The spectra were ratioed against background spectra taken at corresponding temperatures prior to subtracting a horizontal baseline to adjust the lowest absorbance (located in the region 2700–2550 cm^{-1}) to zero for each spectrum.

A program for carrying out the data analyses were implemented in 386-MATLAB on an IBM compatible PC.

Results

IR Spectra and Data Structure. The IR spectra are acquired as vectors with the absorbance reported at every 2 cm^{-1} for the region 4000–650 cm^{-1} . Assuming wavelength shifts to be negligible for individual water species in the investigated temperature range, the spectra acquired at the 48 different temperatures can be collected in a data matrix where each row corresponds to a spectrum at a specific temperature and each column to the absorbance at a specific wavelength. Collecting the spectra according to increasing temperature, the data structure is then defined as an absorbance matrix *A* with increasing temperature defining the vertical direction and increasing wavelength the horizontal direction. The matrix maps (numerically) the structural changes in liquid water as reflected in absorbance changes in the mid-IR spectrum.

Figure 1 shows IR spectra of water acquired at 2.0, 49.3, and 96.2 °C, respectively. The overall absorption decreases with temperature. Furthermore, OH stretching (at ca. 3300 cm^{-1}) shifts toward higher frequency with increasing temperature while the association band (at ca. 2100 cm^{-1}) and the libration band (at ca. 750 cm^{-1}) shift toward lower frequency. Shift of the OH bending band (maximum around 1640 cm^{-1}) is difficult to observe from Figure 1. This observation is in line with the result obtained by Ratcliffe and Irish¹¹ on the bending band of H₂O and D₂O. Between 4 and 300 °C they found that the frequency of the maximum intensity did not change within experimental error, i.e. $\pm 2.5 \text{ cm}^{-1}$. However, the OH bending in our spectra shows a decrease in band width at half height from 112 cm^{-1} at 2 °C to 89 cm^{-1} at 96.2 °C.

Number of Water Species. Our first goal is to determine the number of water species that are necessary and sufficient in order to describe the spectral evolution with increasing temperature. This task can be accomplished by rank analysis¹⁷ of the absorbance matrix *A*.

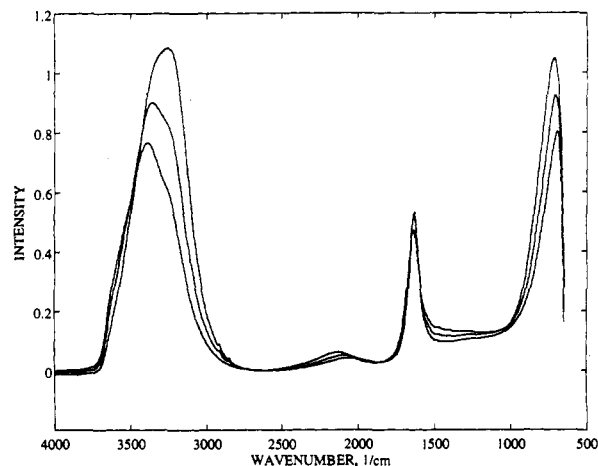


Figure 1. Mid-infrared spectra of water acquired at 2.0, 49.3, and 96.2 °C by means of attenuated total reflection (ATR).

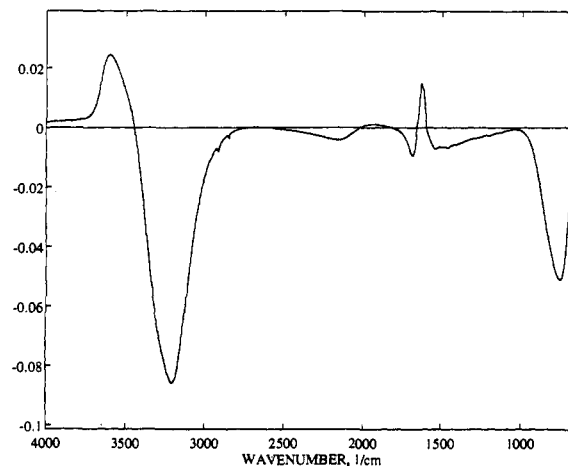


Figure 2. Loadings on the first partial-least-squares (PLS) component plotted versus wavenumber for the acquired spectra.

Partial-least-squares (PLS) regression^{20–21} of the evolving spectra with temperature as the dependent variable shows that one PLS component accounts for 99.6% of the variance in temperature as well as the centered spectral data. Thus, the spectral variance induced by the increased temperature is well explained by the PLS regression technique. The variations in intensities of the IR spectra with temperature are plotted in Figure 2, where the spectral loadings of the component extracted by partial-least-squares (PLS) analysis is shown. Positive intensities represent regions in the IR spectra that increase in intensity with increasing temperature while the opposite is the case for negative intensities. Note that in Figure 2 all spectral bands are separated into subregions increasing or decreasing with temperature. For instance, the loading plot indicates that the combination band (2400–1800 cm^{-1}) contains contributions from two structures having shifted peak position and opposite changes in concentration with temperature. As the low-frequency peak increases and the high-frequency peak decreases, the measured peak shifts toward lower frequency as already observed in Figure 1. Note, however, the increased intensity revealed in the middle of the OH bending band (ca. 1640 cm^{-1}) reflecting the narrowing of the OH bending band with increasing temperature noticed above.

The loading plot (Figure 2) reveals some wavenumbers with no change in absorbance with increasing temperature. Such

(18) Kvalheim, O. M.; Liang, Y.-z. *Anal. Chem.* 1993, 64, 936.

(19) Liang, Y.-z.; Manne, R.; Kvalheim, O. M. *Chemom. Intell. Lab. Syst.* 1994, 22, 229.

(20) Wold, S.; Ruhe, A.; Wold, H.; Dunn, W. J., III *Stat. J. Sci. Stat. Comp.* 1984, 5, 735.

(21) Martens, H.; Næs, T. *Multivariate Calibration*; John Wiley and Sons: Guildford, U.K. 1989.

isosbestic points are located at 3460, 2030, 1655, and 1595 cm^{-1} . This indicates an equilibrium between two structures in water.

The interpretation of water as a closed two-component equilibrium mixture finds support in the large explanatory power of the first PLS component (99.6%) for the spectral variation. The absorbance spectrum $\mathbf{a}(T)$ of a two-component equilibrium mixture acquired at a temperature T can be described as a linear combination of the spectra $\{s_i, i = 1, 2\}$ of the contributing species and an error term \mathbf{e} :

$$\mathbf{a}(T)^t = \sum_{i=1}^2 c_i(T) s_i^t + \mathbf{e}^t \quad (1)$$

Superscript t (transpose) is used to imply row vectors in contrast to column vectors. Equation 1 assumes that wavelength shifts and changes in absorptivities are negligible for the individual species in the investigated temperature range. The noise term expressed as a residual spectrum \mathbf{e} is also assumed to be independent of temperature. If this is the case, the absorbance is only a function of the concentrations $\{c_i(T), i = 1, 2\}$. If the system is closed, the concentrations sum to a constant k , i.e. $c_1(T) + c_2(T) = k$. Solving for $c_2(T)$ and substituting into eq 1 gives:

$$\mathbf{a}(T)^t = c_1(T)(s_1^t - s_2^t) + k s_2^t + \mathbf{e}^t \quad (2)$$

Equation 2 shows that centering of the absorbance at each wavelength eliminates the term $k s_2^t$ and therefore the whole absorbance matrix can be described by the vector of evolving concentrations, $c_1(T)$, and the difference spectrum $(s_1^t - s_2^t)$. This proves that the variation pattern of a two-component closed equilibrium mixture can, except for noise, be described by one latent variable for centered data.

The observations supporting a two-component mixture model at the expense of a single-component (continuum) model for water can be summarized as follows: (i) the presence of isosbestic points, (ii) one PLS component accounting for 99.6% of the spectral evolution with temperature, (iii) the narrowing of the OH bending band with increasing temperature, and (iv) the large drop in total absorbance from 2 to 96.2 °C.

False isosbestic points can result from wavelength shifts for a single-component liquid. This can hardly be the case for water since the intensities at all the isosbestic points for the resolved spectra are almost perfectly linearly correlated to the measured intensities. Furthermore, the observed narrowing of the OH bending band with increasing temperature contradicts the hypothesis of a single-component liquid. Rather, band broadening would be expected in this case. The decrease in total absorbance, approximately 30%, accompanying a temperature rise from 2 to 96.2 °C is one order of magnitude too large to be explained in terms of the density change of 4% for water for this temperature rise. Thus, the evolving pattern of the infrared spectrum of water upon heating appears to rule out the possibility of explaining liquid water as a single-component structure.

Is there any possibility that liquid water contains more than two species? One PLS component would still explain the evolving pattern if a single water structure dissociates into several distinct structures, i.e. A transforms into B + C + ... over the whole temperature range. In such a case, the proportions between the fragments B, C, ... are the same and correlation analysis alone is not able to unravel the true picture. The narrowing of the OH bending band suggests that this is not the case since it appears that the "high-temperature" liquid water structure has a simpler structure than the "low-temperature" one. This picture becomes clearer after resolution of the evolving infrared spectra. Another possibility is that we can have two groups of water structures where the structures within a group are so similar that they are indistinguishable by infrared analysis. In this latter case, it still make sense to regard water as composed of two different structures.

Concentrations Determined by Sequential Rank Analysis. If water is a mixture of two species, eq 1 shows that the absorbance $a(T, \lambda)$ at any wavelength λ and temperature T is the sum of the contribution from each species, i.e.

$$a(T, \lambda) = c_1(T) s_1(\lambda) + c_2(T) s_2(\lambda) \quad (3)$$

Equation 3 shows that for selective wavelengths, i.e. regions where a single species is absorbing, the concentrations of that species can be found. In the absence of selective wavelengths, first-order differentiation of eq 3 with respect to λ can be performed to create selective wavelengths. Thus,

$$\partial/\partial\lambda a(T, \lambda) = c_1(T) \partial/\partial\lambda s_1(\lambda) + c_2(T) \partial/\partial\lambda s_2(\lambda) \quad (4)$$

At absorbance maxima (or minima) of one species, its contribution is zero to the first-order derivative and the evolving concentrations of the other species can be directly obtained at the corresponding wavelengths. The problem is to locate the spectral maxima. Equation 4 shows that at wavelengths corresponding to spectral maxima for either of the species in a two-component mixture, the rank of the first-order derivative of the uncentered spectra is reduced from 2 to 1. The rank is equal to the number of species contributing to a wavelength region. However, it is not possible to estimate rank from a vector and thus it not possible to observe rank reduction in vectors either. We need at least two vectors to observe a rank reduction from 2 to 1. The maxima can be obtained by making one of the following assumptions: (i) the presence of at least two absorbance maxima for each species (together they define a matrix) or (ii) local symmetry around absorbance maxima of the individual species. In the former case, the concentration profiles at different maxima for one species can be identified by their perfect correlation except for noise. In this work, we use the latter assumption for extracting concentration profiles.

Assuming that species 2 has a local maximum at wavelength λ_{max} and that the spectrum of the analyte is symmetric just around the maximum, the following relation is obeyed:

$$ds_2(\lambda)/d\lambda|_{\lambda_{\text{max}-1}} = -ds_2(\lambda)/d\lambda|_{\lambda_{\text{max}+1}} \quad (5)$$

By combining the derivatives at the wavelength just before and just after a local peak maximum for analyte 2, the following vector is obtained:

$$\mathbf{v}_{\text{comb}} = d\mathbf{a}(\lambda)/d\lambda|_{\lambda_{\text{max}-1}} + d\mathbf{a}(\lambda)/d\lambda|_{\lambda_{\text{max}+1}} \quad (6)$$

Insertion of eq 4 in eq 6 and then using the symmetry property expressed by eq 5 shows that \mathbf{v}_{comb} is proportional to the concentration profile c_1 of species 1. Thus, the sub-matrix consisting of the column at the spectral maxima of analyte 2 and the sum of the column just before and just after the maximum, has rank one. Accordingly, a procedure starting with $j = 2$ and proceeding in steps of one until $j = M - 1$ for analysis of the sub-matrices consisting of column j in the derivative matrix $d\mathbf{A}/d\lambda$ and the sum of column $j - 1$ and column $j + 1$ in $d\mathbf{A}/d\lambda$ should show local spectral maxima or minima of either of the pure species in an evolving two-component mixture. This procedure, which was recently developed in our laboratory, is called sequential rank analysis.¹⁹

Sequential rank analysis on the uncentered first-order derivatives for the region 1655–1610 cm^{-1} gave the graph shown in Figure 3. The plot shows the logarithm of the second eigenvalue using the column j , the combination of the columns $j - 1$ and $j + 1$ defined by eq 6, and the corresponding combination of columns $j - 2$ and $j - 2$. The latter was included to obtain better noise reduction and thus sharper minima in the rank analysis. The rank analysis revealed three minima in the evolving second eigenvalue at 1645, 1632, and 1620 cm^{-1} . In order to reveal which of these minima correspond to spectral minima or maxima of the two water structures, the matrix \mathbf{A} was augmented with

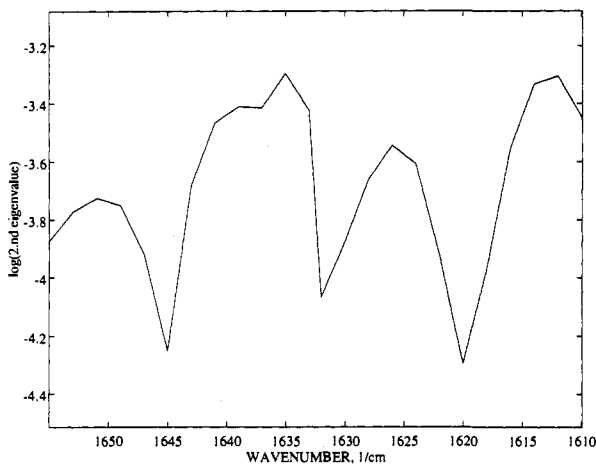


Figure 3. Results of sequential rank analysis applied to the evolving first-order differentiated spectra of water for the temperature range 2–96 °C. The graph shows the logarithm of the second evolving eigenvalue.

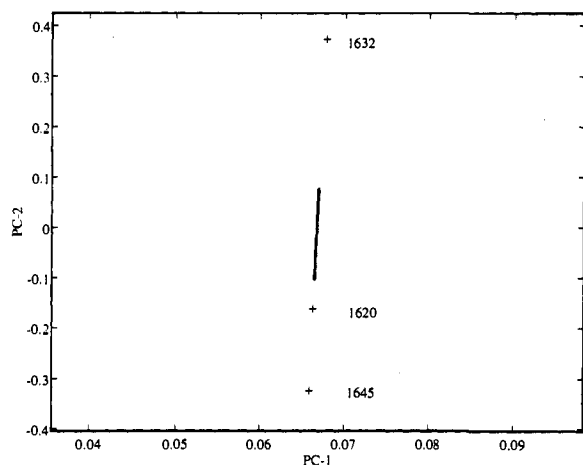


Figure 4. Latent-projective graph for the normalized evolving spectra of water. The labeled points correspond to the differentiated spectra at the minima revealed by sequential rank analysis (see Figure 3).

these three differentiated concentration profiles. Every concentration profile (column of **A**) was then normalized to unit absorbance and the resulting matrix decomposed by principal component analysis. The result of this procedure is plotted in a latent-projective graph¹⁸ as shown in Figure 4. Because of the normalization to constant absorbance, the concentration profiles map a straight line in this graph. The concentration profiles located at the extremes of this line correspond to the pure species, while the concentration profiles plotting between these extremes represent concentration profiles obtained for mixtures. It follows that the differentiated spectra at 1645 and 1632 cm⁻¹ represent the evolving relative concentrations of the pure species.

The evolving concentrations at 1645 and 1632 cm⁻¹ for the differentiated spectra are plotted as a function of temperature in Figure 5.

Resolution of the Infrared Spectra. With the relative concentration profiles of the two water structures available, the spectra can be resolved by least squares. According to eq 1, **A** can be expressed in terms of the concentration $\{c_i\}$ and spectral $\{s_i\}$ profiles

$$\mathbf{A} = \sum_{i=1}^2 c_i(T) s_i + \mathbf{E} = \mathbf{C} \mathbf{S} + \mathbf{E} \quad (7)$$

Spectra and concentration profiles for the evolving mixture are here collected in the two matrices **C** and **S**. Similarly the residual spectra are collected in the residual matrix **E**. A least-squares calculation provides the spectra as

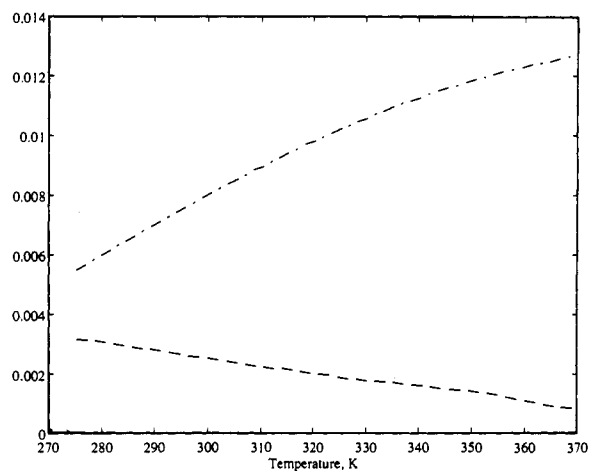


Figure 5. Evolving concentrations for the two water structures obtained at 1632 and 1645 cm⁻¹ of the first-order differentiated spectra. The increasing concentration profile is obtained at 1645 cm⁻¹, while the decreasing concentration profile is obtained at 1632 cm⁻¹.

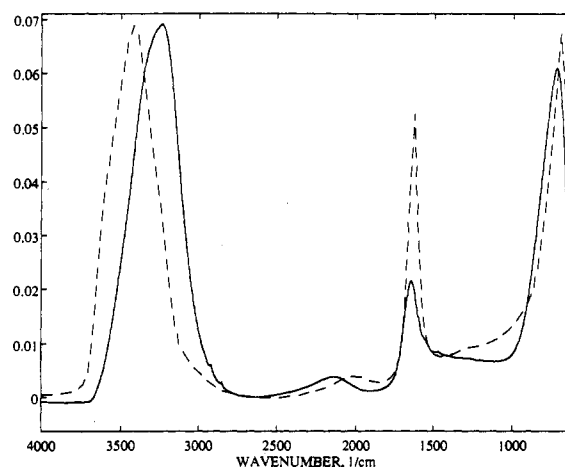


Figure 6. Resolved infrared spectra of the two water structures scaled to unit absorbance.

$$\mathbf{S}' = (\mathbf{C}'\mathbf{C})^{-1}\mathbf{C}'\mathbf{A} \quad (8)$$

The resolved spectra normalized to unit absorbance are shown in Figure 6. The dotted spectrum corresponds to the concentration profile increasing with temperature in Figure 5, i.e. the structure with least H bonding character. This spectrum has its OH stretching maximum at approximately 3410 cm⁻¹, while the other one has its maximum at approximately 3240 cm⁻¹. This difference is in agreement with an interpretation of the two water structures as expressing different H bonding character. The results are in qualitative agreement with the results of Hare and Sorenson.¹³

The spectra show combination bands with maxima at approximately 2020 cm⁻¹ (dotted) and 2150 cm⁻¹, both slightly asymmetric with a high-frequency tail. This agrees with the results of Walrafen et al.,⁵ showing a high-frequency component decreasing with increasing temperature and a low-frequency component increasing with increasing temperature. However, Walrafen et al.⁵ needed three Gaussian bands in order to obtain an acceptable fit.

In the OH bending infrared region of water, the maximum of the species with least H bonding character (dotted spectrum in Figure 6) is positioned at lower frequency than the spectrum corresponding to the species with strongest H bonding character, 1632 and 1645 cm⁻¹, respectively. This result contrasts the findings of Walrafen et al.,⁵ who report the maximum of the decreasing species at the lower frequency. Table 1 in ref 5 shows that the frequency of the maximum of this band decreases with

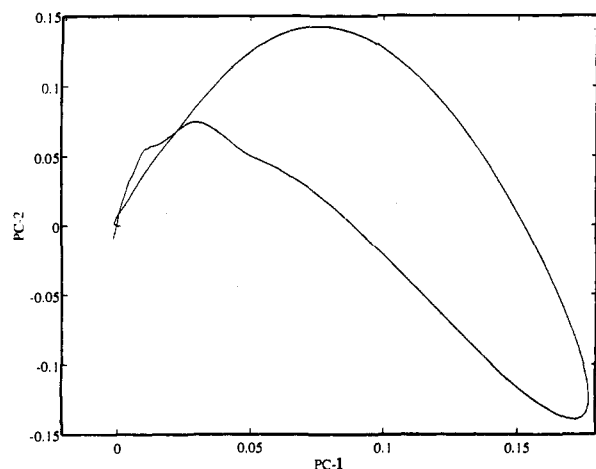


Figure 7. The 1450–1800 cm^{-1} region of the evolving spectra plotted on the two major principal components.

increasing temperature, in correspondence with the behavior of the maximum of the OH bending band in the present work. In order to observe a decreasing peak frequency of this band, the component increasing with temperature should be at the lower frequency. The result indicates stronger H bonding character in the decreasing species, as a stronger H bonding character means that the bending mode of water is more inhibited and thus requires more energy than a less H associated one. The band of the species with most pronounced H bonding character is broader than the band of the species with less H bonding character. This is in agreement with the result obtained by Walrafen et al.⁵ (see Figure 1 in ref 5). This observation suggests either a wider distribution of species at lower temperatures than at higher or that the dominant structure at lower temperature has more than one type of H bonds. The results of the PLS correlation analysis above are in favor of the latter interpretation since it is rather unlikely that different water structures should coexist in the same proportions over the whole temperature range investigated. Our result can be further confirmed by plotting the spectral evolution with increasing temperature on orthogonal components obtained, e.g., by principal component analysis. Such a latent-projective graph¹⁸ is shown in Figure 7. The figure shows that the start and end of the composite OH bending band almost coincide, confirming an interpretation of a narrow band completely overlapped by a broader band.

The libration band region (peak maximum around 750 cm^{-1}) is not discussed because this represents the limit of the operation range of the zinc selenide crystal and MCT-detector used.

Residual Spectra. The concentration profiles were recalculated by doing a least-squares analysis using the resolved spectra normalized to unit absorbance in eq 7. The concentrations thus obtained are plotted versus temperature in Figure 8. The residual matrix was subsequently calculated from eq 7. Figure 9 shows the reconstructed (from CS') and measured spectra at 2, 49.3, and 96.2 °C. The agreement between measured and estimated spectra is excellent. Only the OH stretching region shows some minor deviations. Together with the interpretation above, this result shows that water may well be interpreted as consisting of two different groups of structures, both involved in H bonding, but one group of species with more pronounced H bonding character than the other.

Enthalpy and Entropy Change. The presence of isobestic points (Figure 2) shows that the two kinds of water structures have no or minor changes in the molar infrared absorptivity with changing temperature. This observation further shows that the enthalpy and entropy change can be calculated from the evolving concentration profiles for the transformation from the structure with the strongest H bonding character to one with less H bonding

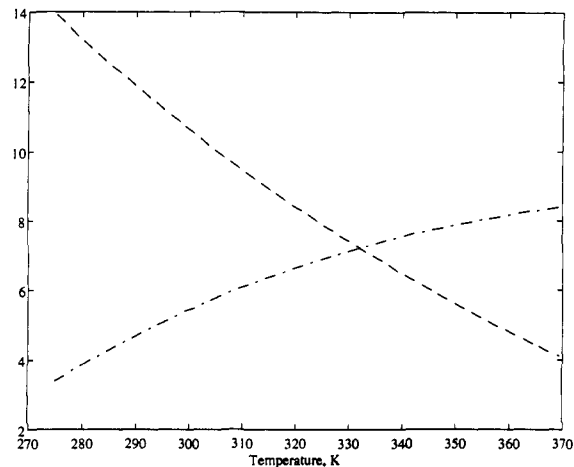


Figure 8. Evolving concentrations for the two water structures obtained at 1632 (decreasing concentration profile) and 1645 cm^{-1} (increasing concentration profile) of the first-order differentiated spectra.

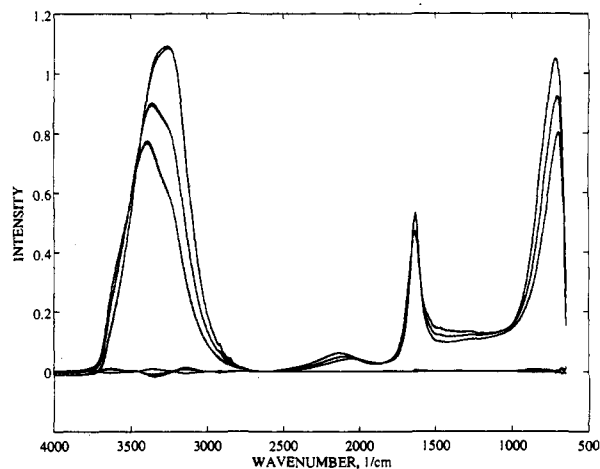


Figure 9. Reconstructed and measured mixture spectra of water at 2.0, 49.3, and 96.2 °C. At baseline the differences between measured and estimated spectra are shown.

character. Following the reasoning of Benson and Siebert,⁹ we assume that half a H bond is broken per water molecule through the transformation from one water structure to the other. The equilibrium can thus be expressed as



The spectra were scaled to the intensities of the isobestic points and the concentration profiles were recalculated by least-squares analysis. According to the equilibrium expressed by eq 9, $\ln K$ was calculated from the recalculated concentration profiles and plotted versus $1000/T$. The result is shown in Figure 10. The enthalpy was calculated as 2.2 kcal mol^{-1} and the entropy change as 7.3 $\text{cal mol}^{-1} \text{K}^{-1}$. These values are in excellent agreement with the results derived by Benson and Siebert⁹ by a completely different approach. Furthermore, our result for the energy of the H bond of 4.4 kcal mol^{-1} falls well inside the range of values reported in the literature,^{14,22–24} covering the interval of 1.9–6.73 kcal mol^{-1} . It is, however, slightly lower than the lower limit of 4.9 kcal mol^{-1} postulated by Benson and Siebert.⁹

Increasing the difference in net number of H bonds between the two water structures results in a too high entropy change, while a decrease gives a too small entropy change.

(22) Aliotta, F.; Vasi, C.; Malsano, G.; Majolino, D.; Mallamace, F.; Migliardo, P. *J. Chem. Phys.* **1986**, *84*, 4731.

(23) Stevenson, D. P. *J. Chem. Phys.* **1965**, *69*, 2145.

(24) Senior, W. A.; Verrall, R. E. *J. Chem. Phys.* **1969**, *73*, 4242.

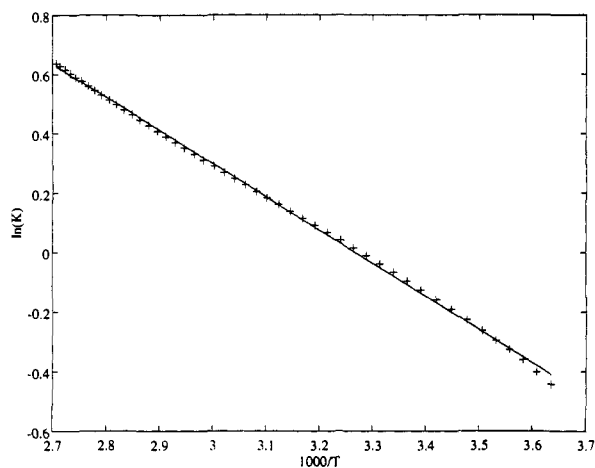
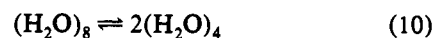


Figure 10. The natural logarithm of the ratio of the evolving concentrations plotted versus the inverse absolute temperature. The enthalpy (slope) corresponds to 2.2 kcal mol⁻¹. The entropy change (the intercept) corresponds to 7.3 cal mol⁻¹ K⁻¹.

Structure of Liquid Water. The result that approximately half a H bond is broken per water molecule during transformation from one structure to the other can provide some crucial clues regarding the nature of the two structures in liquid water. For instance, the simplest model of water as consisting of long chains of H bonded water molecules at low temperatures and then breaking down into smaller fragments is rejected by our results. In order to break half a H bond per water molecule on the average, we need to postulate very long chains of water molecules breaking up into dimers. The energy of vaporization (9.9 kcal mol⁻¹) shows that such a model is not possible. As pointed out by Benson and Siebert,⁹ the enthalpy of melting ice (1.4 kcal mol⁻¹) suggests that on the average one quarter of a H bond is broken upon the transformation from ice to liquid water at 0 °C. Benson and Siebert use this observation to postulate cubic octamers where each water molecule shares three H bonds corresponding to a net of 1.5 H bonds per water molecule. In order to account for a higher net amount of H bonds per water molecule, they also postulate the presence of clusters of octamers, for instance, three octamers connected in a symmetric ring through three extra H bonds. This would increase the net to 1.625 H bonds per water molecule. Dissociation of an octamer into two tetramers,

i.e.



provides a structure with one H bond per water molecule. Just as the octamers do, the tetramers can cluster through additional H bonds.

The two types of water structures postulated by Benson and Siebert differ by exactly half a H bond and so represent plausible candidates for the two-component mixture of water. However, as pointed out by Benson and Siebert,⁹ an equilibrium between polycyclic decamers and monocyclic pentamers is just as plausible since these structures produce H bonds with less strain than the octamer/tetramer pair. Equilibria involving several cyclic structures are also possible according to Benson and Siebert,⁹ but they are less probable as they would probably show a more complex variation pattern than that found in our analysis. With our resolved infrared spectra at hand, it should be possible to determine the correct structures by ab initio calculation of infrared spectra for the candidate structures.

Conclusions

Two different approaches to deconvolution of infrared profiles, namely partial-least-squares regression and evolutionary curve resolution, both show that water can be considered as a two-component mixture. The two structures differ by approximately 0.5 in their average number of hydrogen bonds per water molecule. The mid-infrared spectrum of water was resolved by means of an evolutionary curve resolution method developed in our laboratory.¹⁹ The method generates selective infrared absorption bands at absorption maxima for each chemical species by means of first-order differentiation of the infrared profiles. Assuming local symmetry around the absorbance maxima of the individual chemical species, rank analysis applied to the first-order derivative evolving spectra can locate these maxima. Least-squares analysis using the concentrations obtained at these wavelengths of the differentiated spectra provided resolved infrared spectra for the two water structures. With these spectra at hand, researchers can assess the plausibility of proposed water structures by calculating their infrared spectra. This provides the opportunity to make comparisons at the molecular level as opposed to the common practice of using thermodynamic quantities to make inferences about the molecular structure.

Acknowledgment. F.O.L. and J.T. are grateful for financial support from the Royal Norwegian Council for Scientific and Industrial Research (NTNF) and the Norwegian Research Council for Science and Humanities (NAVF), respectively.